

Measuring Light Pollution with a Calibrated High Dynamic Range All-Sky Image Acquisition System

Georg Zotti

Institute of Computer Graphics and Algorithms
Vienna University of Technology
gzotti@cg.tuwien.ac.at

October, 2007

Abstract

Combining series of exposures with different exposure times made with a digital SLR camera and a fish-eye lens allow to create high-resolution images that contain the full dynamic range of daylight, including the Sun, usable as scene background and for skylight illumination computation purposes. These High Dynamic Range (HDR) images can also be calibrated with a luminance meter, so the image data contain meaningful values, and the system becomes a measuring device. At night, long-time exposures can be combined, and the setup, once fine-calibrated with a Sky Quality Meter or another low-level light measuring device, becomes a valuable tool to provide absolute values of sky brightness. Using data from the astronomical literature, false-colour plots of sky luminance can be created that closely match visual estimation of visible stellar magnitudes.

1 Introduction

Similar to professional-grade astronomical CCD cameras, the image sensors of digital cameras are devices that provide linear response to light. On-board image processing, however, often spoils the linearity, creating images that closely resemble film-based photographs. But RAW image data, provided by many cameras, can indeed be evaluated numerically and can be shown to be very well linear, at least in the mid-range between a minimum level (bias,

noise level) and the saturation level. Long-time exposures of the night sky can be used to analyze natural (twilight) and artificial (sky glow due to light pollution) sky brightness pointwise on any point of the sky dome.

2 Related Work

The system described here makes use of the concepts of High Dynamic Range Imaging. *Dynamic Range* in this context means the relation between maximum and minimum luminance in a given scene. Contrary to conventional photographic images, which try to provide an image optimally suited for print on reflective paper or display on a monitor or screen of severely limited dynamic range, HDR imaging attempts to capture the full dynamic range of natural scenes without allowing under- or overexposed image areas. The processing for display on any conventional or also HDR-capable screen can then be performed from the HDR image data. HDR images can also be used as area light sources for illumination of computer graphics scenes. HDR processing methods and many applications for HDR images for computer graphics are extensively described by REINHARD *et al.* [2006].

Our skydome acquisition setup described here is very close to the approach of STUMPFEL *et al.* [2004], also described by REINHARD *et al.* [2006]. They used a setup consisting of a Canon 1Ds digital SLR camera and Sigma 8mm fisheye lens capable of capturing the whole sky (180°). The sky is photographed with a se-

ries of different exposures until all regions in the image have been imaged with no saturated and no underexposed pixels. The Sun is too bright even for the shortest exposure time, so they had to use an ND3 filter (transmission 0.1%), which however caused a colour shift in the images that had to be removed by a colour transform computation. Their approach was targeted towards daylight HDR image acquisition for display as scene background and image-based lighting, but they did not give details about absolute photometric values, and the available HDR images seem not to be calibrated.

3 Creation of HDR Images of the Sky Dome

Our skydome capturing system consists of a Canon EOS 5D digital SLR with 8mm Sigma fisheye lens (originally the f/4.0 EX model improved for Digital SLR, later the f/3.5 EX DG model, which shows less internal reflections), operated in tethered mode via USB connection to a notebook that runs a remote-control application. Typically, every few minutes a skylight capture sequence is triggered which gathers a series of exposures with different exposure time, which are immediately analyzed after download to detect whether additional longer or shorter exposures are required to cover the whole range of luminance values on the skydome, including the solar disk, so that every image area is imaged at least once without over- or underexposure. Given the enormous brightness of the Sun, up to ten images are required per scene, and an ND3 neutral density filter is used as long as the Sun is above the horizon to keep the exposures in the range manageable by the camera. The colour shift caused by the ND3 filter has to be removed by a colorimetric correction during image processing. Due to the considerable processing requirements, the RAW images are then combined offline on a more powerful PC into HDR images, which can then be further analysed.

To create our HDR images, we decided to use the PFSTools [MANTIUK *et al.* 2007; PFSTools 2006]. This suite of (mostly) command-line programs, which is still under development, is freely available for download in source code form and is intended to be a toolbox of

small programs that can be chained via UNIX pipes to create, modify, store and display HDR images in several formats. A programming extension towards GNU Octave allows analysis or simple modifications like devignetting or application of specialized filters to HDR images in shell scripts or even from the command line.

The PFSTools also include a program to calibrate the final images with measurements taken with a luminance meter to provide absolute luminance values in units of [cd/m²]. While the PFSTools are capable of finding at least approximate luminance values for unfiltered images by evaluating the EXIF image metadata, the filtered images clearly require correct calibration.

The native image format (.pfs) uses IEEE 754 32-bit floats for each of the channels containing CIE XYZ colour values, resulting in huge HDR image files of 94MB for the skydome images in full resolution, cropped to 2800 × 2800 pixels. Following the observation that typical natural scenes have RGB (or XYZ) values of similar order of magnitude, the Radiance XYZE (.hdr) format, which uses 8 bits per component and a common exponent for the three components (totalling 32 bits per pixel), appears to be a more storage-efficient candidate for the permanent storage of larger numbers of (typical) HDR images.

4 Results and Applications

With the setup described above, several series of afternoons and evening twilights have been captured from a rooftop in the western outskirts of Vienna.

Table 1 shows the results of the imaging run on 2007-08-07. The captures of this day show dramatic cloud scenery with light rays shining through the clouds before a thunderstorm required a break. During twilight, there is only a shortish phase in civil twilight where clouds appear dark. During nautical twilight, urban light pollution (sky glow) reaches noticeable levels and illuminates the clouds. The ND3 filter was removed during twilight, but, by the colorimetric correction mentioned above, no colour shift is visible.

As described by REINHARD *et al.* [2006], HDR images typically have to be tone mapped for display on a conventional device like a monitor or print. Using automatic exposures

Time	00	10	20	30	40	50
14						
15						
18						
19						
20						
21						
22						
23						
0						

Table 1: Sky captures of 2007 August 7. The ND3 filter was removed after 19:20. Rain caused a break from 15:55–17:40. During nautical twilight, urban sky glow (light pollution) takes over cloud and sky illumination with its orange cast. For luminance levels, see figure 1.

in conventional photography or (correctly applied) tone mapping for processing HDR images usually results in images that look “correctly exposed”, so that most of the image shows scene details that also are visible to an observer adapted to the same observing conditions. This however is only one application of HDR photography. As mentioned previously, HDR photography is intended to capture the full scene luminance, and so images store valuable data that can also be evaluated numerically.

4.1 Measurements of Sky Luminance and Colours

Figure 1 (a) shows the zenith luminance (black dots) for 2007-08-07 (see images in Table 1) derived from averaging a small area around the zenith, and a curve of the solar altitude during that afternoon (red). From the data plot it can be seen that the zenith luminance during the day varies by a factor of 10 until the Sun is at an altitude of about $h_{\odot} = 5^{\circ}$. During twilight, luminance levels rapidly drop by more than 5 orders of magnitude, and zenith luminance already almost reaches minimum after nautical twilight ($h_{\odot} = -12^{\circ}$). During the twilight phase, the instantaneous capturing of the whole sky is certainly the greatest advantage over sequential scanning methods that require at least several minutes to scan the skydome with automatically pointed measuring heads, even if those may provide more accurate results. In Vienna, public illumination of most areas is reduced to half power already at 23:00 since 2007-02-01, and this drop is very noticeable in the light curve. Still, the amount of sky glow due to urban illumination is significant.

The luminance values for daylight and twilight skies derived from evaluating the HDR photographs closely match measurements made with a Minolta LS-110 luminance meter, which however can only measure down to 0.01 cd/m^2 , and also match sky luminance values given by SCHAEFER [1989-93], indicating the usability of this approach.

The HDR images can also be evaluated with a different aspect in mind: colorimetric measurements, and the development of sky colour dependent on solar altitude. Such studies have been performed by atmosphere physicists, *e.g.*, LEE [1994], who compares chromaticity val-

ues derived from data taken with a spectroradiometer to chromaticities taken from scanned film slides and notes the speed advantage of the photographic method, even if accuracy usually is not as high.

Figure 1 (b) shows curves for sky colour in the CIE xy colorimetric diagram. The sky colour is shown to be largely constant during the day, but during twilight, the blueness rapidly increases. The suburban night sky is dominated by the colours of street lamps. It must however be noted that the spectral sensitivity of the camera system should be better known to produce reliable results.

To compare our measurements with unpolluted sky conditions, a series of twilight and night shots taken in the Libyan desert on 2006-03-28 was processed with the same tools. The zenith luminance data start at sunset with values comparable to European skies, but rapidly decreases towards values of only 1/10 of those, confirming the splendid visual impression of a dark desert sky. From the darker site, the Milky Way and especially zodiacal light is excellently visible (Fig. 2). To achieve exposure values that can be meaningfully analysed under so dark skies, exposure times of several minutes are required. The numerical values achieved from the images closely match data for optimal conditions (see Figure 5 and Table 3).

4.2 Measurements of Nocturnal Light Pollution with HDR Images

A negative effect of human civilisation is the ever increasing level of wasteful outdoor illumination which leads to an artificial increase of diffuse nocturnal sky luminance. This *light pollution* has been observed for decades with concern by astronomers, but increasingly the effects of light pollution has also become the subject of environmentalists who study the effects of artificial illumination on animals and also humans, and develop possibilities in decreasing the waste of energy caused by carelessly designed or installed luminaires, examples of which are shown in Figure 4 [CINZANO 1997; LANDESUMWELTANWALT and UMWELTANWALTSCHAFT 2003].

Nocturnal sky luminance values are obviously of interest for astronomers, but several units of measurement are in use concurrently,

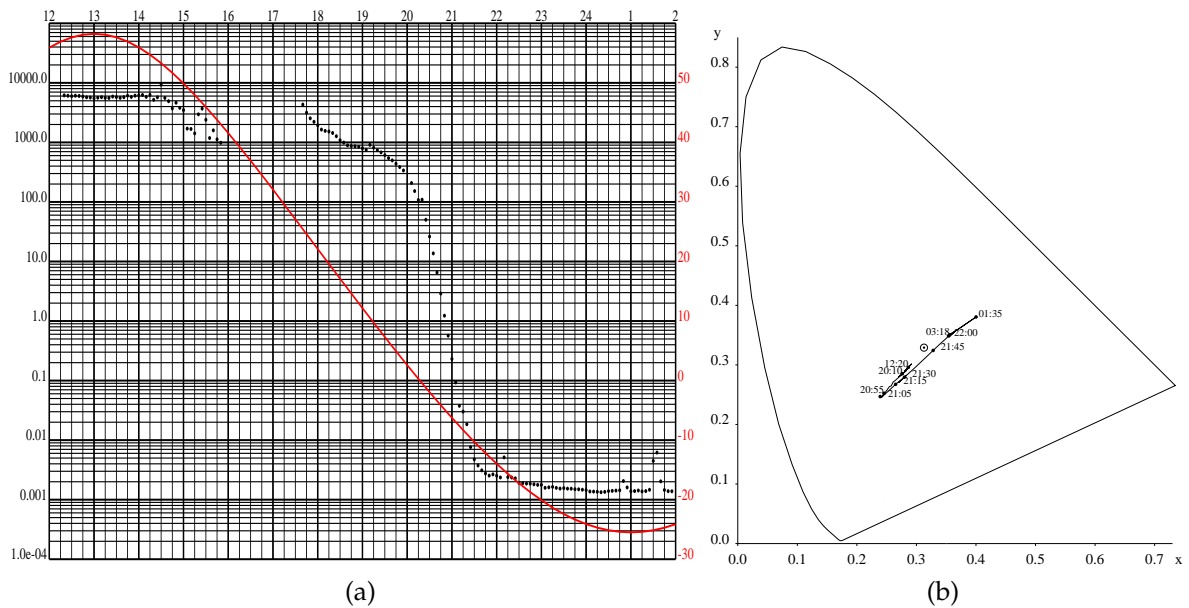


Figure 1: Zenith data measured from the HDR sequence of 2007-08-07: (a) luminance (black dots, logarithmic scale [cd/m^2] on the left) and solar altitude (red curve; labels in degrees on the right side). Clouds cause the jittered values from 14:30–18:15, and rain the break from 15:55–17:40. (b) Colours in the CIE xy chromaticity diagram. Values with zenith clouds during the day (which move sky chromaticity towards the neutral point) have been removed to show clear-sky data only. At night, clouds further pull the chromaticity towards that of street lamps, else the final position is reached with the end of nautical twilight.

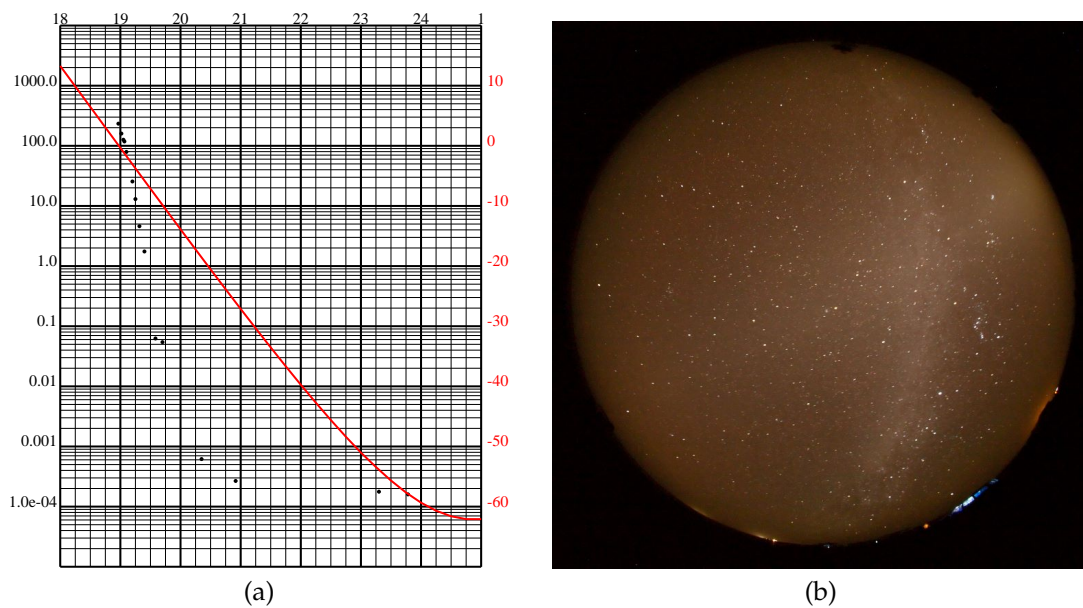


Figure 2: (a) Twilight curve in the Libyan desert. (b) Dark sky with Milky Way and Zodiacal light.



Figure 3: Lake Bled on 2007-10-05 during the day and at night. A high number of glaringly powerful globe lamps emit light wastefully into the sky. (Photographs by the author)

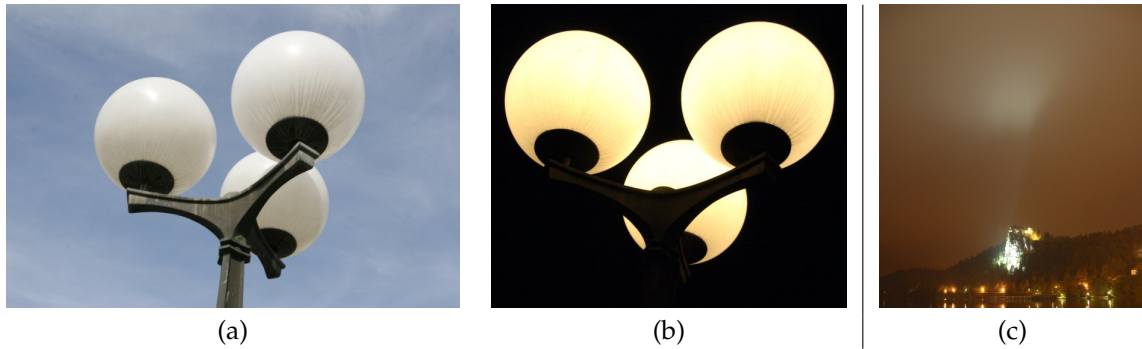


Figure 4: Examples of bad lighting: (a-b) Unshielded globe lamp. More than 50% of the light is emitted directly into the sky, absorption by dirt and occlusion by the lamp pole prevent the light from reaching the ground, where it would be useful. (b) Illumination of the historical Bled castle, Slovenia. Improper luminaire orientation causes a high amount of light spill into the sky. (Photographs by the author)

making the comparison of studies somewhat difficult. Figure 5 tries to combine several of the frequently found units or pseudo-units. The x axis provides logarithmic scales of $[\text{cd}/\text{m}^2]$ and the older unit Nano-Lambert ($[\text{nL}]$, dotted lines), where $1\text{cd}/\text{m}^2 = \pi \times 10^5 \text{nL}$.

Yet another scale is the number of stars of 10^{th} magnitude per square degree that provides equivalent luminance, S_{10} , with $b [\text{nL}] = 0.22 b [S_{10,vis}]$ [CINZANO 1997, Section 3.1.5].

In his model of artificial night sky illumination, GARSTANG [1986, Eq.(19)] quotes the relation between sky luminance b in Nano-Lamberts (nL) and the unit of $\text{mag}/\text{arcsec}^2$ frequently used in the astronomical literature:

$$b [\text{nL}] = 34.08 \exp(20.7233 - 0.92104 b [\text{mag}/\text{arcsec}^2]) \quad (1)$$

from which, with the relation $b [\text{nL}] = \pi \cdot 10^5 b [\text{cd}/\text{m}^2]$, CINZANO [1997, Eq. (3.24)] derived

$$b [\text{mag}/\text{arcsec}^2] = 12.603 - 2.5 \log_{10} b [\text{cd}/\text{m}^2] \quad (2)$$

This relation is presented in the lower straight line in Figure 5.

GARSTANG [1986] also quotes a relation between sky luminance b [nL] and limiting visual stellar magnitude V , given by WEAVER [1947],

$$V = \begin{cases} 7.930 - 2.171 \ln(1 + 0.1122b^{1/2}) & (b \leq 1479 \text{ nL}) \\ 4.305 - 2.171 \ln(1 + 0.001122b^{1/2}) & (b > 1479 \text{ nL}) \end{cases} \quad (3)$$

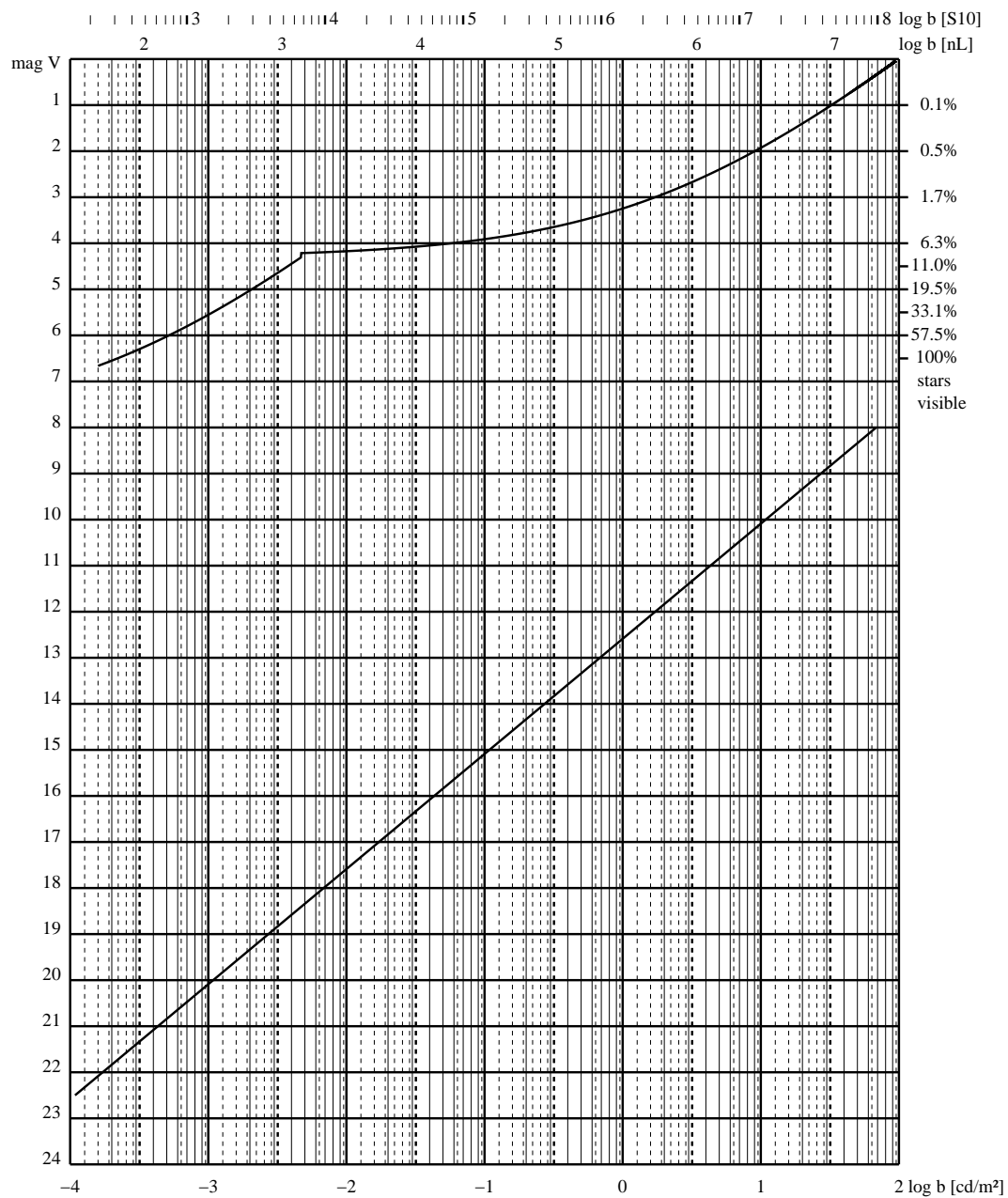


Figure 5: Limiting stellar magnitude *vs.* sky luminance, after GARSTANG [1986]. The horizontal axis is sky luminance b , given in units of $[\text{cd}/\text{m}^2]$ (also called nits, lower scale) and also in two other frequently used units: Nano-Lamberts (nL, upper scale, dotted vertical lines), and the S_{10} scale which represents the number of stars of 10th magnitude per square degree that give equal luminance (tick marks near numbers). The vertical axis shows photometric (V) stellar magnitude mag_V . The lower straight line connects sky background in the $[\text{mag}/\text{arcsec}^2]$ scale with the other photometric units (eq.1), and the upper curve shows the limiting stellar magnitudes visible with the unaided eye, depending on sky background luminance (eq.3). The bend at $0.005 \text{ cd}/\text{m}^2$ marks the transition from mesopic to scotopic (dark-adapted) vision.

Table 2: Visibility of the Milky Way depending on average Polluted Sky Luminance, after CINZANO [1997].

Sky Luminance		Description
[nL]	[cd/m ²]	
1150	$3.7 \cdot 10^{-3}$	invisible
500	$1.6 \cdot 10^{-3}$	visible near zenith, rest immersed in grayish background
150	$5 \cdot 10^{-4}$	reduced contrast, details lost
80	$2.5 \cdot 10^{-4}$	brilliant if high, not visible on horizon
64	$2 \cdot 10^{-4}$	best conditions

Table 3: Zenith Sky Luminance values after CINZANO [1997]

Source	Zenith Values [$\cdot 10^{-6}$ cd/m ²]	
	Typical	Minimal
Zodiacal Light	91 (70–126)	56
Integrated starlight	77 (21–213)	21
Diffuse galactic light	6–14	5.6
Airglow (min)	35	35
Cosmic Background	<0.7	<0.7
Total	217	118

which is shown in the upper part of Figure 5. From the curve it can be seen that truly dark-adapted vision only takes over at luminance values lower than 0.005 cd/m^2 , and only at these low values the abundant numbers of dim stars begin to become visible, as indicated on the right scale (after CINZANO [1997, Tab. 4.2]). Under optimal conditions, the limiting visual zenith magnitude can be around mag 6.5, which is however beyond all hope near larger cities.

Evaluating Zenith Data

Comparing zenith luminance data from the HDR image analysis (Figure 1) with the upper curve in Figure 5, it can be seen that the limiting zenith magnitude for the light-polluted suburban skies measured by the HDR capture system was slightly better than about mag 5, which matched a visual estimate: the Milky Way was barely visible near the zenith. CINZANO [1997] lists visibility estimates for the Milky Way depending on sky luminance (Tab. 2), and the description for 500 nL supports the results of the measurement.

A strongly light polluted sky is comparable to the sky luminance at Full Moon (1400 nL after SCHAEFER [1989-93]). Very slowly, also through activities of the International Dark-Sky Association [Darksky], public conscious-

ness and legislative seems to be evolving towards the use of light fixtures that directs light towards the ground, where it is potentially useful, instead of into the sky, and generally the use of more energy-efficient lights, although there is still a long way to go. CINZANO [1997] studied light pollution and listed natural contributions of night sky luminance values, given in Table 3. From this data, the darkest skies to be expected should show zenith values around $1.2 \dots 2.2 \cdot 10^{-4} \text{ cd/m}^2$, values that also appear in the analysis of images taken in the Libyan desert (Figure 2).

All-Sky Evaluation

Recently, DURISCOE *et al.* [2007] presented an extensive high-precision study of sky luminance by light pollution in US national parks, using a science-grade CCD camera on a robotic telescope mount to acquire highly accurate light pollution data by scanning a multitude of directions in the sky over a period of about 35 minutes. From the point measurements, they produced fisheye-like plots of the sky, colour-coded in units of [mag/arcsec²].

The fisheye HDR images in this present work, after de-vignetting, can be evaluated and colour-coded in a similar way. As reference measurements, visual estimates by experienced observers and measurements with a Sky Quality Meter (SQM) [UNIHEDRON], a dedicated electronic low-light measuring device that provides direct sky background brightness on the [mag/arcsec²] scale, have been used. The latter two matched well with the connecting relations shown in Figure 5. It however turned out that the photographic estimates were slightly too optimistic (*i.e.*, the sky appeared too dark).

The reason for this discrepancy can be found in the fact that the Y luminance channel data provided by the PFSTools represents the photopic (daylight) sensitivity function of the human visual system, while visual limiting magnitudes obviously involve the scotopic (night) sensitivity function, which has its peak shifted towards shorter wavelengths. The spectral sensitivity of the SQM as described by CINZANO [2005] is much higher in the short wavelength range than that of the photopic sensitivity function, but also does not provide astronomically representative values, because it does not represent any astronomically standardized filter system. Also, its wide aperture angle poses a problem given that the horizon is considerably brighter in light polluted areas, so any comparison must take this wide angle into account.

A multiplicative correction factor as large as 1.4 (0.37 mag) has been found to be required for the sky luminance near Vienna by comparing the average of a large area in the image representing the area measured by the SQM – weighted by the SQM’s angular response given by CINZANO [2005] – to the single measurement value given by the SQM. This factor, which lies well within the range derived by CINZANO [2005], depends on the spectral emission characteristic of the street lamps involved, and Vienna’s high amount of mercury vapour lamps include a significant blue component where the SQM is sensitive.

To describe naked-eye visibility of the night sky around cities, we prefer to show limiting visual magnitude following the function given by GARSTANG [1986] (eq.3), instead of the more technical unit of [mag/arcsec²], and the plots in Figures 6–7 are colour-coded accordingly.

5 Discussion

The HDR capture setup with a D-SLR camera described in this paper was originally intended to provide high-quality daylight sky captures usable for image-based lighting in a high-quality rendering system and as ground truth against which a skylight simulation shall be compared. Its application towards attempting high-precision measurements also of the night sky has been developed as side-effect, but seems to be well usable. Compared to incidence measurements like the SQM or a luxmeter, the method presented here provides high

angular resolution, allowing the identification and quantification of emitters on the horizon.

On the downside, the required processing capabilities are not negligible, but processing can be performed by a powerful notebook also in the field.

The *flat field* images for devignetting have been made by photographing the inside of a globular milk glass lamp-shade on a cloudy day with no direct solar illumination. Still better results would be expected from using an integrating sphere with images with and without filters to also identify a likely stronger filter effect near the horizon circle, where the light rays pass the filter at an oblique angle and thus would be filtered more strongly. Colour calibration would then have to be performed depending on radial distance from the image center.

The absolute luminance levels were calibrated with a Minolta LS-110 luminance meter, which however has a minimum sensitivity of 0.01cd/m². By using longer exposure times, the fisheye sky capture system reaches considerably lower luminance levels. Calibration measurements with a Sky Quality Meter finally allowed the determination of nocturnal sky brightness. While the fully automated capture system is usable to capture night skies inside a city downtown about 0.001cd/m², rural skies can only be measured using “bulb” exposure times of several minutes. Also, the spectral sensitivity of the camera would have to be determined to relate the “instrumental magnitudes” to astronomical magnitudes in standardized filter systems to further improve accuracy.

For more reliable results about the average quality of observing sites, many more systematic capture series would be required, which will also have to be correlated to systematic weather observations. Also, the influence of snow on urban and rural night sky luminance would be an interesting subject.

Acknowledgements

The remote control application was implemented by Franz Daubner. This work was supported by the Austrian Science Fund (FWF) under contract number P17558 and the *Hochschuljubiläumstiftung der Stadt Wien* by project number H-1085/2004.

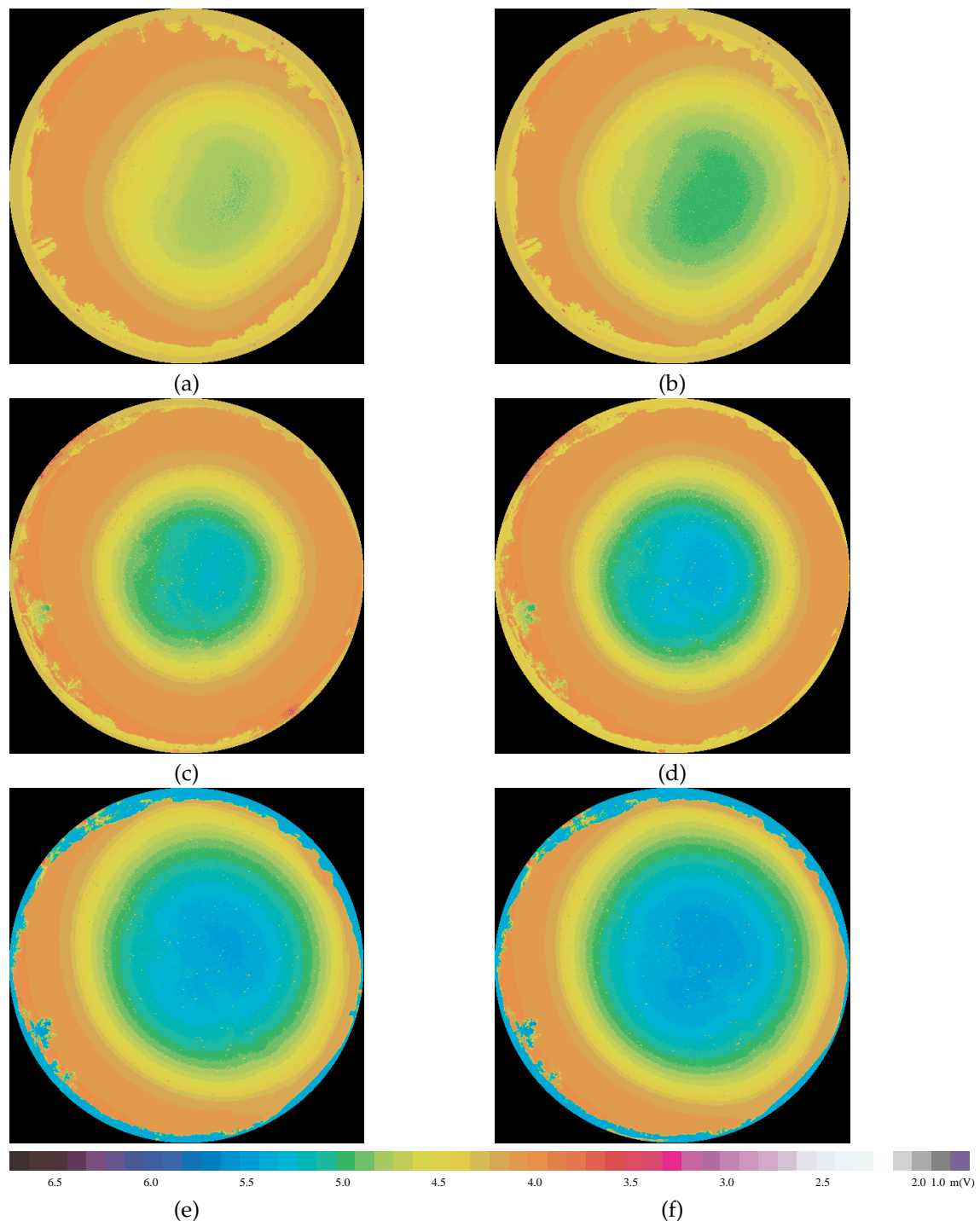


Figure 6: Sky luminance given as plots of maximum visible magnitude: Effect of reduced public illumination. (a) Night sky in suburban Vienna, on 2006-07-05, 23:55CEDT (b) 15 minutes later, after reduction of public illumination, the sky gets notably darker. (c) Night sky on Sophienalpe, close to Vienna, on an average day (2007-08-22) (d) On the same location 30 minutes later. After reduction of public illumination, the sky gets notably darker. (e) Night sky on Sophienalpe, on a good day (2007-09-14) (f) On the same location 45 minutes later. After reduction of public illumination, the sky got notably darker.

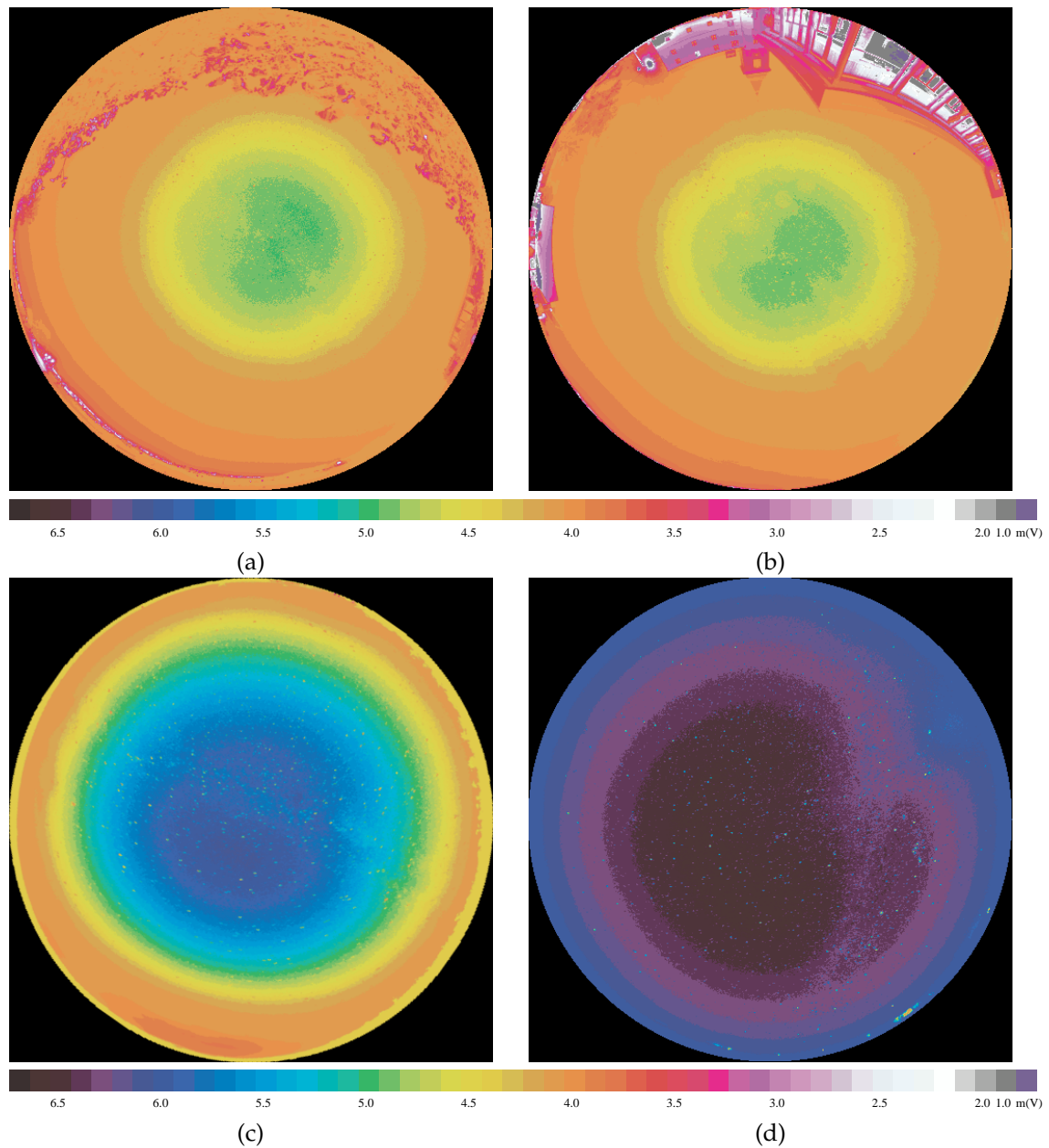


Figure 7: Sky luminance given as plots of maximum visible magnitude: (a) Night sky at Cobenzl/Vienna, 2007-08-22, at midnight (b) Night sky at Kahlenberg/Vienna, 2007-08-22, after midnight (c) Night sky near Großmugl, Lower Austria, approx. 20km from Vienna, 2007-08-22. The glow of Vienna is on the southern (low) horizon. (d) Night Sky in the Libyan desert, 2006-03-29. Astronomer's dreamland!

A Skydome Capture System Based on PFStools

This appendix describes our setup for High Dynamic Range (HDR) skydome image acquisition using advanced consumer-grade digital cameras and extensions to free software which has been used for the results presented in this paper.

A.1 Skydome Capture System

Our camera is a Canon EOS 5D, which is equipped with a full-size CMOS sensor (full-size means identical in size to conventional 35mm film, *i.e.*, 24×36 mm). Our lens was originally a Sigma 8mm f/4 like the one used by STUMPFEL *et al.* [2004], but a newer model which has been improved especially for digital cameras. One reported improvement was a smaller divergence of the light beam which decreased vignetting, because vertical incidence is more important for electronic sensors than for film. However, internal reflections of the solar image created disturbing artifacts. The lens was later replaced by the further improved Sigma 8mm f/3.5, which does not show these artifacts. To avoid excessive heat buildup that could lead to more noise, the camera can be wrapped in a first-aid safety blanket (aluminized mylar, also known as “space blanket”), although exactly for the short exposures in daylight we did not experience a significant improvement with this professional-grade camera.

Canon provides a programming toolkit which we used to create a program that can take a sequence of exposures with different exposure times. The program is available for download at our institute’s website [DAUBNER 2007]. The images are downloaded to the controlling notebook, and a function based on `dcrw` (see section A.2) is used to analyze the raw image for over- and underexposure in the circular sky area. The first exposure time has to be preset, and additional exposures are done typically 2 f-stops apart (4 times longer or shorter), until the whole sky zone has been imaged with no under- and overexposed areas. Most images are taken at f/4, but capturing the sun requires f/16 to prevent overexposure. Like STUMPFEL *et al.* [2004] we also found the necessity for a Kodak Wratten #96 ND3.0 neu-

tral density filter to reduce the intensity of direct sunlight during daytime, which however causes a colour shift that has to be corrected later in the processing pipeline. The filter must be removed after sunset for captures of twilight and the night sky.

A.2 Decoding RAW Images from Consumer Cameras

Camera vendors use different RAW formats for their cameras, which are usually closely dependent on the respective sensors and fulfill the purpose of providing the full sensor resolution, which is more than the 8 bits of common JPEG images. It seems impossible for the user to really get access to the original ADC values from the sensor, because at least the error map processing (averaging out single bad pixels) is done immediately by the onboard camera software. A great help in converting all the different raw formats to a single file format is `dcrw` [COFFIN 2007], which is provided in source code, supports over 250 camera models and can write 16-bit `.ppm` and `.tiff` files that are either totally unprocessed (so they show the Bayer filter pattern and raw, unscaled colours), or just interpolated and white-balanced images that are as close to linear as possible. It also includes functionality to process bad pixels which develop as process of detector aging via an external error map file that includes pixel coordinates and their failure dates, so that also images taken before the failure date can be processed again without “correcting away” the pixel that still worked nominally at that date. Also the subtraction of a dark frame is possible, and, with a compile switch, even whitepoint calibration from a Macbeth Color Checker chart can be performed.

A.3 Creation of HDR Sky Images with PFStools

To create the HDR images, we use the PFStools [MANTIUK *et al.* 2007; PFStools 2006], a suite of (mostly) command-line programs intended as research and production toolbox of small programs that can be chained via UNIX pipes to create, modify, store and display HDR images in several formats. A programming extension towards GNU Octave allows analysis or simple modifications like devignetting or application

of specialized filters to HDR images in shell scripts or even from the command line.

The program `pfshdr_calibrate`, which is part of the PFSTools, not only finds the sensor response curve for digital cameras required to properly create HDR images from a series of exposures with different exposure times, but even finds out approximate absolute luminance values in $[\text{cd}/\text{m}^2]$ from the exposure and image data. For JPEG images, the PFSTools authors estimate the accuracy of this evaluation to be near 8%, which is usually good enough for most applications in computer graphics, even for the application of luminance-dependent tone-mapping algorithms. True calibration by absolute measurements with a luminance meter is possible with `pfsabsolute`.

Finding Sensor Response

Combining truly linear images into HDR images would be trivial. Unfortunately, consumer-grade cameras usually deliver images which have been processed from the original linear sensor response to simulate classical film behaviour. Frequently, high luminance levels in the original 12-bit sensor data are stronger compressed in the final 8-bit images in order to enhance the low and mid-tones, and “image styles” can further influence the response mapping. But also the “raw” images can show nonlinearity by anti-blooming gates that practically reduce sensitivity near the saturation level. Creating HDR images from such nonlinear images requires the reconstruction of the response mapping from scene luminance to image value. Several methods have been proposed [*e.g.*, DEBEVEC and MALIK 1997; ROBERTSON *et al.* 1999]. The PFSTools by default use the method of ROBERTSON *et al.* [2003].

In order to create a response curve, the only requirement is a series of photographs of a static scene which should not even show very high dynamic range, with identical settings except for exposure time. The authors recommend to slightly defocus the image, so that sharp contrast edges pose no problem in case of even minimal camera shake between exposures.¹ As further recommendation we shall

¹ Several HDR creation toolkits include programs to align the images before combination to the HDR image. For the PFSTools, a program `pfsalign` has been presented [TOMASZEWSKA and MANTIUK 2007], but has not been

note that glare around saturated areas in these images likewise leads to unusable results and *must* be avoided. So, the best image sequence includes frames that barely show anything and frames that contain only slightly saturated areas. Of course, a regular rectilinear lens has to be used with images completely filling the sensor area, or, rectangular image areas can be cut with `pfs_cut`, if only fisheye images (with black corners) are available.

`pfshdr_calibrate` originally supported only JPEG files, so the author of this work contributed a small program to read exposure parameters from RAW images (Fig. 8).

First, exposure data for all image files are read from the image files and written into a parameter file (`hdrgen` script), then `pfshdr_calibrate` analyzes and matches the response of corresponding pixels, and writes a response file for the respective camera. Example:

```
$ dcraw2hdrgen *.cr2 > img.hdrgen
$ pfsinhdrgen img.hdrgen |
  pfshdr_calibrate -v -b 16 -s camera.response
```

The `-b 16` is applicable for RAW files only, for JPEG files, `jpeg2hdrgen` and `-b 8` should obviously be used.

The authors then recommend to analyze the resulting response curve visually with:

```
$ gnuplot
gnuplot> plot "camera.response" with dots
```

The result for our camera in `.cr2` and `.jpg` formats and the (irrelevant by motive) calibration image is shown in figure 9. The curves for the RAW files overlap and are smooth and practically identical, while the curves for JPEG files show the typical S-profile of processed images.

The response curve can now be used for HDR generation of this and other image sequences taken with the same camera and the same white balance and sensitivity settings.

Creating Ordinary HDR Images

A series of raw images in `.cr2` format is first again processed with `dcraw2hdrgen` to extract exposure data into a configuration file. From this file and the response data file, a regular HDR image is generated with the sequence

integrated so far, and preliminary substitutes are recommended on the PFSTools website.

```

#!/bin/bash
#
# This file is a part of PFS CALIBRATION package.
# -----
# Copyright (C) 2004 Grzegorz Krawczyk, <gkrawczyk@users.sourceforge.net>
#
# This program is free software; you can redistribute it and/or modify
# it under the terms of the GNU General Public License as published by
# the Free Software Foundation; either version 2 of the License, or
# (at your option) any later version.
#
# This program is distributed in the hope that it will be useful,
# but WITHOUT ANY WARRANTY; without even the implied warranty of
# MERCHANTABILITY or FITNESS FOR A PARTICULAR PURPOSE. See the
# GNU General Public License for more details.
#
# You should have received a copy of the GNU General Public License
# along with this program; if not, write to the Free Software
# Foundation, Inc., 59 Temple Place, Suite 330, Boston, MA 02111-1307 USA
# -----
# This program by Georg Zotti <gzotti@cg.tuwien.ac.at>, derived from jpeg2hdrgen
#
# $Id: dcrw2hdrgen,v 1.2 2006/08/22 18:34:04 gkrawczyk Exp $

LC_NUMERIC=POSIX          # ensure dot is used as the decimal separator
export LC_NUMERIC

LC_ALL=POSIX              # apparently this is necessary on Gentoo
export LC_ALL

DCRAW="dcrw -i -v"        # program for extracting exposure info from "raw" images

TEST_DCRAW='which dcrw';
if [ "$TEST_DCRAW" = "" ]; then
    echo "Program 'dcrw' is required to run this script."
    echo "Install appropriate software, for example from:"
    echo "http://www.cybercom.net/~dcoffin/dcrw/"
    exit 1;
fi

#Note: Double backslash MUST be put in front of each $ sign
AWK_PROGRAM='cat <<EOF
BEGIN {
    exposure="";
    aperture="";
}

END {
    if( aperture=="")
        aperture=1;

    if( iso_speed=="")
        iso_speed=100;

    if( exposure=="")
        printf("unrecognized raw format!\n");
    else
        print exposure " " aperture " " iso_speed " 0";
}

/^Shutter: ([\ ]?([0-9]*\.[0-9]*) sec/ {
    if (substr(\2, 1, 2)=="1/")
        exposure = substr(\2, 3);
    else
        exposure = 1/\2;
}

/^Aperture: F\|f\|([0-9]*\.[0-9]*)/ {
    aperture = substr(\2,3);
}

/^ISO speed: ([0-9]*\.[0-9]*)/ {
    iso_speed = \2;
}

EOF`

while [ "$1" != "" ]; do
    EXPOSURE_INFO=`$DCRAW $1 | awk "$AWK_PROGRAM"`
    echo $1 $EXPOSURE_INFO

    shift
done

```

Figure 8: dcrw2hdrgen, a script contributed to the PFSTools to read exposure data from RAW images supported by dcrw

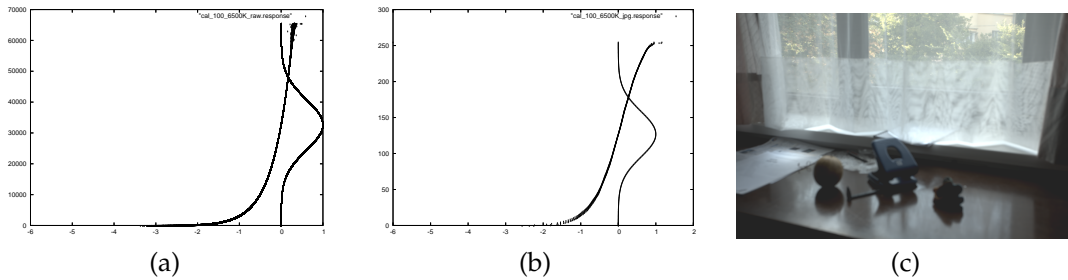


Figure 9: Camera response curves for Canon 5D, Serial #1831204000, at ISO 100, colour temperature 6500 K, (a) for raw 12-bit format (b) for JPEG format. The Gaussian curves show the most reliable range of pixels. (c) The scene, tonemapped with `pfstmo_durand02`

```
$ dcraw2hdrngen *.cr2 > img.hdrngen
$ pfsinhdrngen img.hdrngen |
  pfsHDRcalibrate -v -b 16 \
    -f camera.response |
  pfsoutrgbimg img.hdr
```

where in this case an HDR image in Radiance RGBE format [LARSON and SHAKESPEARE 1998] is created. Note that the OpenEXR format [INDUSTRIAL LIGHT AND MAGIC 2003] is not capable of storing the full range of daylight luminance values including the solar disk, and `pfsoutexr` would emit a warning message for such images. For our evaluation, we use the native PFS format, which uses IEEE 754 32 bits floating point numbers per pixel and channel, and stores CIE XYZ values. The images require lots of disk space (94MB for an image in full resolution of the EOS-5D, cropped to the square including the circular fisheye image area), but could be converted to other formats or scaled with `pfsresize` if required.

Correction of Lens Effects

Both Sigma 8mm fisheye lenses show slight *chromatic aberration*, which can be corrected in `dcraw` with the switch `-C 0.999 1.0001`.

The geometric radial imaging characteristic of fisheye lenses can be adequately described by a function $r = \alpha \sin(\beta\theta)$ with angle from image center θ and parameters α and β unique to a given lens [KUMLER and BAUER 2000]. These values can be derived, *e.g.*, from measuring stellar images and comparing the positions with catalog data. For the Sigma f/4.0 lens, $\alpha = 14.7, \beta = 0.54$ have been derived by KUMLER and BAUER [2000]. More accurate general formulations have been presented, *e.g.*, by VAN DEN HEUVEL *et al.* [2006] or SCHWALBE [2005].

The radial brightness falloff (*vignetting*) depends on the respective lens and field stop value. Ideally, to fix vignetting (and several other defects) in CCD images made with optical systems providing rectilinear images, a homogeneous white surface is imaged as *flat* calibration image, and the scene image of interest (*science frame*) is then divided pixel-wise by the normalized flat [BERRY and BURNELL 2000]. A method to correct vignetting in photographs from consumer cameras has recently been proposed by D'ANGELO [2007], who uses it for stitching HDR panoramic images.

A *flatfield image* for a fisheye image would have to be made inside a homogeneously lit white sphere known as *integrating sphere*. A fisheye image of this sphere ideally would be a homogeneously lit circle, but would typically rather show the vignetting pattern instead. As approximative solution, a globular lamp shade made from milk glass can be put over the fisheye lens in a location with unblocked horizon under a cloud-covered sky without direct sunshine, and series of exposures are then taken with all aperture settings used for the production images.

The images are processed into regular PFS files, but then normalized with the added program `pfsnormalize` (Fig. 10).

With such an image, the sky images can be flat-fielded using `pfsflatfield` (Fig. 11).

Camera Colour Calibration

The Kodak Wratten #96 ND3.0 neutral density filter is not so neutral, but causes a colour shift that requires a white balancing step. The program `dcraw` is also capable of such colour correction: A Macbeth Digital ColorChecker® SG card was photographed in the institute's

```
#!/bin/bash

# script calling pfsocetavelum with a fixed octave script.
# This script scales the Y channel so that its maximum is 1.
# Images can then be used to Flat-Field other images.

# Works with pfstools, the HDR suite by MPI.
# G. Zotti, 2007-08-07

pfsocetavelum 'Ymax=max(max(Y)) ;
              fprintf(stderr, "pfsnormalize: Ymax=%11.9f, scaling image\n", Ymax);
              Y /= Ymax ; '
```

Figure 10: pfsnormalize: Setting maximum luminance to 1.

```
#!/usr/bin/octave -q
#
# This file is an addon to the PFSTOOLS package.
# author Georg Zotti, <gzotti@cg.tuwien.ac.at>
#
# Example usage: pfsin scene.pfs | pfsflatfield Flat.pfs | pfsout scene-flattened.pfs

if( length( argv ) != 1 )
    error( "pfsflatfield: Expecting exactly one parameter, the flatfield PFS image" );
endif

flat = pfsopen( argv{1} );
flat = pfsget ( flat);

pin = pfsopen( "stdin" );
pin = pfsget ( pin );

if ((pin.rows != flat.rows) || (pin.columns != flat.columns))
    error("pfsflatfield: Flat and Image Frame Size Mismatch!");
endif

pout = pfsopen( "stdout", pin.rows, pin.columns );

## Copy channels and tags from the source to destination stream
pout.channels = pin.channels;
pout.tags = pin.tags;
pout.channelTags = pin.channelTags;

[Yflat _xflat _yflat] = pfstransform_colorspace( "XYZ", flat.channels.X, \
        flat.channels.Y, flat.channels.Z, "Yxy" );

[Y _x _y] = pfstransform_colorspace( "XYZ", pout.channels.X, \
        pout.channels.Y, pout.channels.Z, "Yxy" );

Y = Y ./ Yflat ; # Octave allows element-wise division without looping!

[pout.channels.X pout.channels.Y pout.channels.Z] = \
        pfstransform_colorspace( "Yxy", Y, _x, _y, "XYZ" );

pfsput( pout );
pfsfclose( pin );
if( exist( "pout" ) != 0 )
    pfsfclose( pout );
endif

pfsfclose ( flat );
```

Figure 11: pfsflatfield: Pixel-wise division of image data.

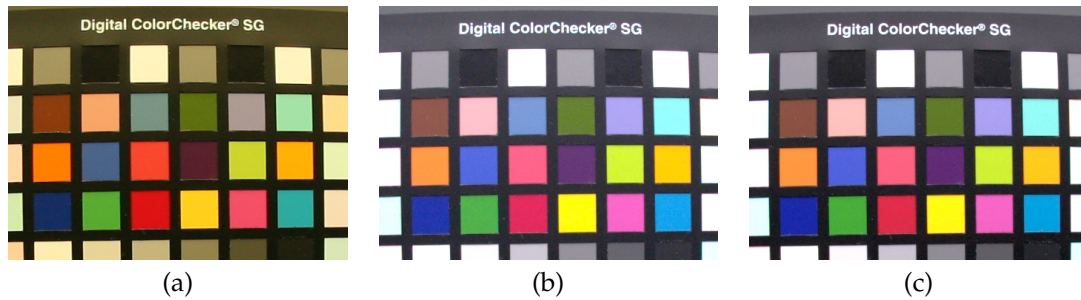


Figure 12: Removing colour shift caused by Kodak Wratten #96 ND3.0 “neutral density” filter: (a) filtered image, exposed 180 seconds, without calibration. (b) filtered image after calibration. (c) unfiltered image (exposed 1/8s), after calibration.

lightbox under D65 illumination through the fisheye lens, with and without filter. The coordinates of the classical 24 Macbeth Color Checker patches were entered in the `dcraw` source and the program recompiled with the `-DCOLORCHECK` switch. The command

```
$ dcraw -v <filename>.CR2
```

then provides the required values for achieving white balanced images. The colour shift of filtered images can now be removed with a regularly built `dcraw` with the correct scaling values via the sequence

```
$ dcraw -r <values> <filename>.CR2
```

Figure 12 shows the exposures through the filter before and after white balance correction and an unfiltered image for comparison. The result is not absolutely identical, but very close to an image taken without filter and likewise processed with the self-calibrating colour check. By default, `pfsindcraw` of the `PFS`Tools calls `dcraw` with the “camera white balance” option. A patched version of this script is shown in figure 13.

To better evaluate the filter characteristic, a transmission spectrum should be recorded with a calibrated spectroradiometer.

Absolute Calibration

While `pfshdrcalibrate` finds approximate scene luminance values from the EXIF exposure data in JPEG images, luminance for both filtered and unfiltered RAW images must be adjusted with `pfsabsolute`. Correct absolute values are also required for a smooth transition of filtered and unfiltered images during twilight and are also important in some tone mapping algorithms.

The simplest way to achieve absolute calibration is to load the HDR image into `pfsview` and read the Y value of a spot close to the image center (where vignetting is still negligible, if the image has not been flat-fielded) that has also been measured in the real scene with a luminance meter. The command to add in the chain is then

```
$ pfsabsolute <measured_value> <img_value>
```

Typically, the values should be in the same order of magnitude for unfiltered JPEG exposures, because via `pfshdrcalibrate` approximately correct luminance values have been derived from ISO range, exposure time and aperture value. Comparative measurements with a Minolta LS-110 luminance meter showed however the necessity of a scale factor of 3.1 ± 0.3 to scale the luminance values in the PFS files resulting from RAW images combination. The presence of filters of course must be corrected in this way.

The real filter factor for the ND3 filter was reconstructed from the luminance difference between filtered and unfiltered exposures made in the lightbox. It is more correctly an ND3.18 filter with transparency of about 1/1700. The zenith brightness values now reconstructed from filtered and unfiltered exposures after calibration closely match those values given by SCHAEFER [1989-93, p.321], with an error estimate of typically less than 10%.

After this step, the HDR file now contains corrected luminance values in $[\text{cd}/\text{m}^2]$ and can be used as sky radiance map in a global illumination renderer or evaluated for other purposes.

```

#!/bin/bash
#####
# Wrapper for dcrw.
# Convert digital camera RAW files to 16bit PPMs.
#
# this is a stub with basic functionality
# PATCH BY GZOTTI: ADDED $PFSINDCRAW_DCRAWPAR
#####

if test -z $1 || test "$1" = "--help" || test "$1" = "-h"; then
cat <<EOF

Read an image in a camera RAW file format supported by
DCRAW and write pfs stream to the standard output as
if read from 16bit ppm file (no gamma correction,
white balance from camera if available).

Usage: pfsindcraw <file> [<file>...]

See the man page for more information.

If \PFSINDCRAW_DCRAWPAR is set, it is used as parameters to dcrw,
and it must include white balance commands.

EOF
    exit 1
fi

# This avoids problems if not calling via mkSky, and keeps original behaviour.
if [ -z "$PFSINDCRAW_DCRAWPAR" ] ; then
    echo >&2 "Using Camera White Point "
    PFSINDCRAW_DCRAWPAR="-w"
fi

if ! which dcrw 2>/dev/null 1>/dev/null; then
    echo -n >&2 "pfsindcraw: dcrw program not found. "
    echo >&2 "Check if it is installed and can be found in the PATH."
    exit 1;
fi

if ! which pfsinppm 2>/dev/null 1>/dev/null; then
    echo -n >&2 "pfsindcraw: pfsinppm program not found. "
    echo >&2 "Check if pfstools are compiled with netpbm support."
    exit 1;
fi

#Arguments used for all images passed to pfsindcraw
global_arguments=""
if test -n "$1"; then
    while test "${1:0:1}" = "-"; do
        case $1 in
            *)
                echo >&2 "No option is implemented at the moment."
                exit 1;
            esac
            global_arguments="$global_arguments $1"
            shift
        done
    fi

while test "$1"; do
    file_pattern=$1

    dcrw -c -m -4 $PFSINDCRAW_DCRAWPAR $file_pattern | pfsinppm - 2> /dev/null | \
        pfstg --set "FILE_NAME=${file_pattern}" --set "LUMINANCE=RELATIVE"

    shift
done

```

Figure 13: Patched version of pfsindcraw to feed arguments to dcrw via environment variables.

HDR Skylight Script

The capture program creates file names in the format `SKY_YYYYMMDD_HHMMSS_seq.CR2`, with date and time of the first image in a sequence taken from the controlling notebook's clock, and `seq` a sequence number: `00` for the first image, and numbers `+nn` and `-nn` for longer and shorter exposures, respectively. The script `mkSky` (Fig. 14) is used to process these series of `.cr2` images into a `.pfs` HDR file, where `pfscut` is used to trim the unused image area and create a square image. The flatfield command should be added in the command sequence as soon as a flatfield image has been created.

The combination of several Canon 5D RAW images takes several minutes and significant amounts of memory. On an Athlon™ 64 3500+ processor, the observed memory footprint was about 1.7GB.

To process a whole directory of captures, *e.g.*, a full day, we can use the obvious shell command sequence:

```
$ for f in SKY_20070807_*_00.CR2
do
    echo $f
    mkSky `basename $f _00.CR2`
done
```

Masking Empty Pixels

Ideal fisheye images consist of an image circle inside a black rectangle, which we have trimmed already into a square during the HDR image generation above. Bias, dark current or stray light from a low sun cause some unwanted illumination in the corner zones, which can be trimmed away easily with a tiny add-on script, `pfscircle`, that calls the general GNU Octave interface `pfsoctavelum` and can be added anywhere in the command sequence (Fig. 15).

Tone Mapping

The HDR image can be used for purposes like image-based lighting, where the HDR data obviously provide far superior results over conventional photographs [REINHARD *et al.* 2006]. HDR monitors have been presented already, but are extremely expensive. For presentation of the HDR images on conventional screens and also in print, the dynamic range of daylight scenes, which can well be 6 orders of magnitude for images including the Sun, has to be

compressed again by *tone mapping*, which ideally is used like an auto-exposure feature on a camera that produces conventional images, so that twilight and night scenes are visible even if luminance levels are about 6 orders of magnitude lower than average daylight scenes. The dynamic range of scenes without the Sun is obviously by far smaller.

The PFSTools include several implementations of tone mapping algorithms [PFStmo 2007]. Tone mappers are not aware of the black image circle but could be confused by stray light in the outer circle, and may on the other hand change this outer area, so `pfscircle` should be used before and after the tone mapper. Example use:

```
$ for f in *.pfs ; do
    pfsin $f | pfscircle |
    pfstmo_fattal02 | pfscircle |
    pfsout `basename $f .pfs`_fattal02.jpg
done
```

Zenith Brightness Evaluation

The GNU Octave interface `pfsoctavelum` can be used for a variety of extensions to the PFSTools, of which we give a final example.

To record zenith brightness values for a full day capture sequence, a central box in the image (in the case below, the images had been scaled down with `pfssize`, so a 7×7 box was adequate) can be sampled with the following command sequence. Note that the script evaluated by `pfsoctavelum` must obviously not write to `stdout`, where the `pfs` stream is written.

```
$ for f in *.pfs ;
do
    echo -e -n "`basename $f .pfs` \t" ;
    pfsin $f |
    pfsoctavelum \
    'Yavg=0.0; cnt=0 ;
    for y=pin.rows/2-3 : pin.rows/2+3 ;
    for x=pin.columns/2-3 : pin.columns/2+3 ;
        Yavg+=Y(y, x) ;
        cnt++ ;
    endfor ;
    endfor ;
    Yavg/=cnt ;
    fprintf(stderr, "%11.9f\n", Yavg); ' \
    > /dev/null ;
done
```

Similar, but longer scripts have been used to create the false-colour plots of the night sky for Figures 6–7.

```
#!/bin/bash
# script to create one sky HDR image

# Let this variable point to your calibration file
CALIB_FILE=/data/Sky/Cal20070729/cal_1600_6500K_raw.response
# Let this variable point to your flat file
FLAT_FILE=/data/Sky/Flat/Flat_Sigma-8mm_f4.pfs
# chromatic aberration fix for Sigma 8mm f/4 Fisheye images for dcraw
CHROMATIC_ABERR="-C 0.999 1.0001 "

if [ "$1" == "" ]
then
echo "Usage : $0 [-n] [-f] <SKY_DDMMYYYY_HHMMSS> "
echo "Option: -f apply colour match for filtered image "
exit 0
fi

# define chromatic aberration fix, colour and absolute multipliers
# for sRGB with or without filters
# Comparative measurements with Minolta LS-110 indicate a factor 3.1 for RAW images.

if [ "$1" == "-f" ]
then
echo "Creating sRGB Sky HDR image made with ND3 filter"
export PFSINDCRAW_DCRAWPAR="$CHROMATIC_ABERR -v -r 1.846705 1.0 2.213889 1.0 "
export PFSABSOLUTE_FACTOR="334800 63.7"

shift
else
echo "Creating sRGB Sky HDR image made without ND3 filter"
export PFSINDCRAW_DCRAWPAR="$CHROMATIC_ABERR -v -r 2.381668 1.0 1.469678 1.0 "
export PFSABSOLUTE_FACTOR="3.1 1"
fi

if [ -f $1.hdrngen ]
then
echo "Using existing $1.hdrngen"
else dcraw2hdrngen $1_*.CR2 > $1.hdrngen
fi

pfsinhdrngen $1.hdrngen \
| pfsct --left 800 --top 50 --width 2800 --height 2800 \
| pfshdrcalibrate -v -b 16 -f $CALIB_FILE \
| pfsabsolute $PFSABSOLUTE_FACTOR \
| pfsflatfield $FLAT_FILE \
| pfsout $1.pfs
```

Figure 14: mkSky: Capture series to HDR conversion Script

```
#!/bin/bash
# script calling pfsocetavelum with a certain octave script. The image MUST be
# quadratic, or at least wider than high, and a circle of the height of the
# image will be left in the center, the borders will be blackened.
# Works with pfstools, the HDR suite by MPI.
# G. Zotti, 2007-08-07
pfsocetavelum 'Xcent=pin.columns/2 ; Ycent=pin.rows/2; radius = pin.rows/2; \
for y = 1 : pin.rows ; \
angle=asin((Ycent-y)/radius); \
xOff= ceil(cos(angle) * radius); \
for x=1 : Xcent-xOff ; Y(y, x)=0 ; endfor ; \
for x=ceil(Xcent)+xOff : pin.columns ; Y(y, x)=0 ; endfor ; \
endfor ; '
```

Figure 15: pfsocircle: Masking Image Corners

References

- RICHARD BERRY and JAMES BURNELL [2000]: *The Handbook of Astronomical Image Processing*. Willmann-Bell, Inc., Richmond, Virginia, USA. ISBN 0-943396-67-0
- PIERANTONIO CINZANO [1997]: *Inquinamento Luminoso e Protezione del Cielo Notturmo, Memorie Classe di Scienze Fisiche, Matematiche e Naturali*, vol. XXXVIII. Istituto Veneto di Scienze, Lettere ed Arti, Venezia. ISBN 88-86166-48-6
- PIERANTONIO CINZANO [2005]: Night Sky Photometry with Sky Quality Meter. Tech. Rep. 9, ISTIL - Istituto di Scienza e Tecnologia dell'Inquinamento Luminoso (Light Pollution Science and Technology Institute), Thiene, Italy
URL <http://www.lightpollution.it/download/sqmreport.pdf>
- DAVE COFFIN [2007]: Decoding raw digital photos in Linux. online. (accessed July 27, 2007)
URL <http://cybercom.net/~dcoffin/dcraw/>
- PABLO D'ANGELO [2007]: Radiometric alignment and vignetting calibration. In: *Camera Calibration Methods for Computer Vision Systems (Proc. CCMVS 2007)*
URL <http://biecoll.ub.uni-bielefeld.de/volltexte/2007/101>
- Darksky []: International Darksky Association website
URL <http://www.darksky.org>
- FRANZ DAUBNER [2007]: HDR Capture GUI. Software
URL <http://www.cg.tuwien.ac.at/research/publications/2007/daubner-2007-HDR/>
- PAUL E. DEBEVEC and JITENDRA MALIK [1997]: Recovering High Dynamic Range Radiance Maps from Photographs. In: *SIGGRAPH '97: Proceedings of the 24th Annual Conference on Computer Graphics and Interactive Techniques*, pp. 369–378. ACM Press/Addison-Wesley Publishing Co., New York, NY, USA. ISBN 0-89791-896-7. doi: <http://doi.acm.org/10.1145/258734.258884>
- DAN M. DURISCOE, CHRISTIAN B. LUGINBUHL, and CHADWICK A. MOORE [2007]: Measuring Night-Sky Brightness with a Wide-Field CCD Camera. In: *Publications of the Astronomical Society of the Pacific* vol. 119, pp. 192–213
- ROY H. GARSTANG [1986]: Model for Artificial Night-Sky Illumination. In: *Publications of the Astronomical Society of the Pacific* vol. 98, pp. 364–375
- FRANK A. VAN DEN HEUVEL, RUUD VERWAAL, and BART BEERS [2006]: Calibration of Fisheye Camera Systems and the Reduction of Chromatic Aberration. In: H.-G. MAAS and D. SCHNEIDER (Editors), *Proceedings of the ISPRS Commission V Symposium 'Image Engineering and Vision Metrology'*, vol. XXXVI-5. ISSN 1682-1750
URL http://www.isprs.org/commission5/proceedings06/paper/1267_Dresden06.pdf
- INDUSTRIAL LIGHT AND MAGIC [2003]: OpenEXR website
URL <http://www.openexr.com>
- JAMES KUMLER and MARTIN BAUER [2000]: Fish-Eye Lens Designs and Their Relative Performance. In: *Proceedings of the Lens and Optical System Design and Engineering Conference of the SPIE Annual Meeting*, vol. 4093, pp. 360–369. SPIE
- TIROLER LANDESUMWELTANWALT and WIENER UMWELTANWALTSCHAFT (Editors) [2003]: *Die Helle Not: Künstliche Lichtquellen – ein unterschätztes Naturschutzproblem*. Innsbruck, Wien, 2nd edn.
- GREG WARD LARSON and ROB SHAKESPEARE [1998]: *Rendering with Radiance — The Art and Science of Lighting Visualization*. Morgan Kaufmann Publishers, San Francisco, CA. ISBN 1-55860-499-5
- RAYMOND L. LEE, JR. [1994]: Twilight and daytime colors of the clear sky. In: *Applied Optics* vol. 33(21), pp. 4629–4638
- RAFAL MANTIUK, GRZEGORZ KRAWCZYK, RADOSŁAW MANTIUK, and HANS-PETER SEIDEL [2007]: High Dynamic Range Imaging Pipeline: Perception-motivated Representation of Visual Content. In: BERNICE E. ROGOWITZ, THRASYVOULOS N. PAPPAS, and SCOTT J. DALY (Editors), *Human Vision and Electronic Imaging XII*. No. 649212 in Proceedings of SPIE, SPIE, San Jose, USA

- PFStmo [2007]: PFStmo::tone mapping operators. website
 URL <http://www.mpi-inf.mpg.de/resources/tmo/>
- PFSTools [2006]: PFSTools website
 URL <http://www.mpi-inf.mpg.de/resources/pfstools/>
- ERIK REINHARD, GREG WARD, SUMANTA PATTANAİK, and PAUL DEBEVEC [2006]: *High Dynamic Range Imaging – Acquisition, Display, and Image-Based Rendering*. Morgan-Kaufmann Publisher/Elsevier. ISBN 978-0-12-585263-0
- MARK A. ROBERTSON, SEAN BORMAN, and ROBERT L. STEVENSON [1999]: Dynamic Range Improvement through Multiple Exposures. In: *Proc. International Conference on Image Processing, ICIP 1999*, vol. 3, pp. 159–163. IEEE. ISBN 0-7803-5467-2
- MARK A. ROBERTSON, SEAN BORMAN, , and ROBERT L. STEVENSON [2003]: Estimation-Theoretic Approach to Dynamic Range Improvement Using Multiple Exposures. In: *Journal of Electronic Imaging* vol. 12(2)
- BRADLEY E. SCHAEFER [1989-93]: Astronomy and the Limits of Vision. In: *Archaeoastronomy* vol. XI, pp. 78–90
- ELLEN SCHWALBE [2005]: Geometric Modelling and Calibration of Fisheye Lens Camera Systems. In: R. REULKE and U. KNAUER (Editors), *Proceedings of the ISPRS working group V/5 'Panoramic Photogrammetry Workshop'*, vol. XXXVI-5/W8. Berlin. ISSN 1682-1750
 URL http://www2.informatik.hu-berlin.de/sv/pr/PanoramicPhotogrammetryWorkshop2005/Paper/PanoWS_Berlin2005_Schwalbe.pdf
- JESSI STUMPFEL, CHRIS TCHOU, ANDREW JONES, TIM HAWKINS, ANDREAS WENGER, and PAUL DEBEVEC [2004]: Direct HDR Capture of the Sun and Sky. In: *AFRIGRAPH '04: Proceedings of the 3rd international conference on Computer graphics, virtual reality, visualisation and interaction in Africa*, pp. 145–149. ACM Press, New York, NY, USA. ISBN 1-58113-863-6. doi:<http://doi.acm.org/10.1145/1029949.1029977>
- ANNA TOMASZEWSKA and RADOSLAW MANTIUK [2007]: Image Registration for Multi-exposure High Dynamic Range Image Acquisition. In: *Proc. WSCG'2007*. University of West Bohemia, UNION Agency. ISBN 978-80-86943-98-5
- UNIHEDRON []: *Sky Quality Meter (SQM)*. Grimsby, Canada
 URL <http://www.unihedron.com>
- H. F. WEAVER [1947]: In: *Publications of the Astronomical Society of the Pacific* vol. 59, p. 232